Development of human skin equivalents to unravel the impaired skin barrier in atopic dermatitis skin

Eweje, M.O.

CHAPTER 4

Exploring the potential of nurture: 2nd and 3rd generation explant human skin equivalents

Danso MO, van Drongelen V, Mulder A, Gooris G, van Smeden J, El Ghalbzouri A, Bouwstra JA.
J Dermatol Sci. 2015 Feb;77(2):102-9

Abstract

Explant human skin equivalents (Ex-HSEs) can be generated by placing a 4mm skin biopsy onto a dermal equivalent. The keratinocytes migrate from the biopsy onto the dermal equivalent, differentiate and form the epidermis of 1st generation Ex-HSEs. This is especially suitable for the expansion of skin material from which only small fragments of skin can be harvested e.g. diseased skin. We evaluated whether 2nd and 3rd generation Ex-HSEs can also be generated from a single skin biopsy whilst maintaining the epidermal properties of 1st generation Ex-HSEs and native human skin. 2nd generation Ex-HSEs were produced by placing a biopsy from the 1st generation Ex-HSE onto a new dermal equivalent.

Likewise, the 3rd generation Ex-HSEs were generated from a 2nd generation Ex-HSE biopsy.We show for the first time that Ex-HSEs can be passaged to the 2nd and 3rd generation and display similar epidermal morphology and expression of differentiation markers as in native human skin and 1st generation Ex-HSEs except for involucrin. The 2nd and 3rd generation Ex-HSEs also show many similarities with 1st generation Ex-HSEs in lipid properties e.g. presence of all lipid classes, similar fatty acid chain length distribution and lamellar lipid organization. However, some differences arise in increased level of hexagonal lateral packing and a change in ceramide profiling. The changes in specific lipid classes was also accompanied by changes in the expression of the enzymes responsible for their synthesis. The expansion of skin biopsies to the 2nd and 3rd generation Ex-HSEs could be a promising method to expand valuable epidermal tissue to analyze morphological and differentiation parameters in the native epidermis.

Introduction

Human skin equivalents (HSEs) are useful tools for studying the interplay between biological processes in the skin including modeling skin diseases (1-3), wound healing (4-6), cutaneous irritation and toxicity tests (7-9). A novel method of generating HSEs involves placing full-thickness 4mm skin punch biopsies onto a fibroblast populated collagen matrix i.e. dermal equivalent, forming the so called 1st generation explant human skin equivalent (Ex-HSE) (3, 10, 11). We previously demonstrated that the epidermis of 1st generation Ex-HSEs show comparable epidermal stratification and differentiation as the original *ex vivo* skin although not all the stratum corneum (SC) lipid properties could not be reproduced in Ex-HSEs (12). Following this study, the next step was to investigate whether the amount of tissue generated from the 1st generation Ex-HSEs can be further expanded by growing a 2nd generation and even a 3rd generation Ex-HSE. In addition, since the free fatty acids play an important role in the changes in lipid organization in HSEs, we analyze for the first time in Ex-HSEs, the SC fatty acid chain length distribution and degree of saturation quantitatively. Furthermore, we examine the expression of some key enzymes involved in SC lipid synthesis because these factors contribute significantly to the SC skin barrier.

Expansion of epidermal tissue by producing up to three generations of Ex-HSEs can be crucial for analyses that require larger amounts of epidermal tissue, which cannot be harvested from patients with skin diseases. These analyses may include quantitative protein analysis or combining different techniques to study various aspects of diseased skin. By generating a 2nd generation Ex-HSE the total epidermal surface area can be expanded by 40 times compared to the original 4mm skin biopsy (table S1). The 1st generation Ex-HSE was generated from the original biopsy harvested from *ex-vivo* skin. The 2nd generation was produced by harvesting a biopsy from the 1st generation Ex-HSE and implanting this onto a fresh dermal substrate. This approach can be repeated using a biopsy from the 2nd generation Ex-HSE to establish a 3rd generation Ex-HSE (figure S1). During such organ culture, the keratinocytes migrate from the implanted biopsy onto the dermal equivalent, proliferate, differentiate and form an epidermis.

In native human skin, the SC, which is the outermost layer of the epidermis, consists of corneocytes embedded in a lipid matrix and this structure plays an essential role in the skin permeability barrier. The main lipid classes present in native human SC include free fatty acids (FFAs), ceramides (CERs) and cholesterol (CHOL). These lipids form two lamellar phases with repeat distances of approximately 6nm and 13nm referred to as short periodicity phase (SPP) and long periodicity phase (LPP) respectively (13). Within the lipid lamellae, the lipids in native human SC are mainly organized in a dense orthorhombic packing although a fraction of lipids also adopt a hexagonal packing (figure S2) (13-15).

The epidermal stratification, differentiation pattern and SC lipid properties from the 2nd and 3rd generation Ex-HSEs were analyzed in order to investigate whether these properties are similar to those in the 1st generation of Ex-HSE. In addition, the differentiation and barrier properties were also compared to the native human skin.

Materials and methods

Isolation of human dermal fibroblasts

Adult human breast or abdominal skin tissue was obtained from cosmetic surgery after written informed consent, according to the Declaration of Helsinki Principles. Dermal fibroblasts were isolated as described earlier (16) and cultured in Dulbecco's Modified Eagle Medium (DMEM; Invitrogen, Netherlands) supplemented with 5% fetal bovine serum (FBS; Hyclone, UT, USA) and 1% penicillin/streptomycin (Sigma, Zwijndrecht, Netherlands) (17). Passages 2-5 were used for the experiments.

Generation of human skin equivalents

Dermal equivalents were generated as described earlier (16, 18). Briefly, 1mL of a 1mg/mL collagen solution was pipetted into filter inserts (Corning Life sciences, Amsterdam, Netherlands). After polymerization, 3mL of fibroblast populated (0.4×10^5 cells/mL) collagen (2mg/mL) was pipetted on the polymerized collagen. After polymerization, the collagen was cultured submerged (1 week) in DMEM supplemented with 5% FBS, 25mM ascorbic acid (Sigma, Zwijndrecht, Netherlands) and 1% penicillin/streptomycin.

The various generations of Ex-HSEs were generated as described in detail in figure S1. These cultures consist of an explant and its outgrowing area. The explant is defined as the skin biopsy placed onto the dermal equivalent and the outgrowth is defined as the keratinocytes that after migration, proliferate and differentiate to form the main part of the Ex-HSE. After the generation of dermal equivalents, full thickness (FT) 4mm fat free biopsies obtained from breast skin (referred to as the 1st generation explants, age 17-49), were gently pushed onto the dermal equivalents. Subsequently, the HSEs were cultured at the air-liquid interface and cultured for two days with DMEM and Ham's F12 (Invitrogen, The Netherlands) (3:1 v/v), 0.5µg/mL insulin (Sigma, Zwijndrecht, Netherlands), 0.5µM hydrocortisone (Sigma, Zwijndrecht, Netherlands), 1µM isoproterenol (Sigma, Zwijndrecht, Netherlands), 1% penicillin/streptomycin, 25mM ascorbic acid and 5% FBS. During the next two days, the HSEs were cultured in a similar medium as mentioned above with some changes. These included 1% FBS, 0.053µM selenious acid (Johnson Matthey, Maastricht, The Netherlands), 10mM L-serine (Sigma, Zwijndrecht, Netherlands), 10µM L-carnitine (Sigma, Zwijndrecht, Netherlands), 1µM α-tocopherol acetate (Sigma, Zwijndrecht, Netherlands), 25mM ascorbic acid and a lipid mixture of 3.5µM arachidonic acid (Sigma, Zwijndrecht, Netherlands), 30 µM linoleic acid (Sigma, Zwijndrecht, Netherlands) and 25µM palmitic acid (Sigma, Zwijndrecht, Netherlands). For the remaining culture period, the HSEs were cultured with the same composition of the medium with two changes: i) 7µM arachidonic acid and ii) no FBS. The culture medium was refreshed twice a week and the HSEs were cultured for 21 days at 37°C, 90% relative humidity and 7.3% CO_2. At the end of the culture period, the dermal equivalent was covered with a keratinocyte outgrowth from the biopsy (1st generation Ex-HSE). During the harvest of the 1st generation Ex-HSE, a biopsy from the 1st generation outgrowth was placed onto a new dermal equivalent. This biopsy on the new dermal substrate is referred to as the 2nd generation explant and served as the start of the 2nd generation outgrowth. The Ex-HSE was cultured for another 21 days generating the 2nd generation outgrowth. During harvest, the 2nd generation outgrowth was further passaged to

produce the 3rd generation Ex-HSE and cultured for 21 days. The fibroblast donor used to generate a series of 1st-3rd generations Ex-HSEs was kept the same.

Morphology and Immunohistochemistry

Ex-HSEs were fixed in 4% (w/v) paraformaldehyde (Lommerse Pharma, The Netherlands), dehydrated and embedded in paraffin. For morphological analysis, 5µm sections were stained with haematoxylin (2mg/ml) and eosin (4mg/ml). Immunohistochemical analysis for keratin 10 (K10), Ki67, filaggrin, loricrin, involucrin, steroyl-CoA desaturase (SCD) and ceramide synthase 3 (CerS3, analyzed by immunofluorescence) expression was performed as described in supplementary materials and methods.

Lipid extraction/analysis

The SC was isolated from native human epidermis and HSEs as previously described (19). The lipids were extracted from the SC using a modified Bligh and Dyer procedure (20). SC extracts from the outgrowth of 2-3 Ex-HSEs of the same skin donor were pooled. The lipid composition of the explants could not be determined due to insufficient amount of material. Extracts were dried under a stream of nitrogen, reconstituted in chloroform: methanol (2:1) and stored at -20°C. Lipid analysis by high performance thin layer chromatography (HPTLC) and liquid chromatography coupled to mass spectrometry (LC-MS) is described in supplementary materials and methods.

Fourier transformed infra-red spectroscopy (FTIR) and small angle X-ray diffraction (SAXD)

FTIR: Isolated SC sheets were hydrated at room temperature over a 27% NaBr solution for 24 hours. The SC was sandwiched between AgBr windows and mounted into a customized heating/cooling cell. A Varian 670-IR FTIR spectrometer (Agilent technologies, CA, USA), equipped with a broad-band mercury cadmium telluride detector cooled with liquid nitrogen was used to acquire spectra. The spectra were collected in transmission mode, as a co-addition of 256 scans at $1cm^{-1}$ resolution. Each spectrum was collected for 4 minutes at a 1°C interval from 0°C - 90°C, with frequency range of 600-$4000cm^{-1}$ and deconvoluted using half-width of $4cm^{-1}$ and an enhancement factor of 1.7. Bio-Rad Win-IR Pro 3.0 software (Biorad laboratories, MA, USA) was used to analyze the spectra.

SAXD: All measurements were performed at the European synchrotron radiation facility (ESRF, Grenoble) at station BM26B. SAXD patterns were detected with a Frelon 2000 charged-coupled device detector using a microfocus of 25µm x 25µm. The X-ray wavelength and sample-to-detector distance were 0.1033nm and 24cm respectively. The scattering intensity (I, arbitrary units) was measured as a function of the scattering vector q (nm^{-1}) defined as $q= (4\pi\sin\theta)/\lambda$, in which θ is the scattering angle and λ is the wavelength of the x-rays. From the positions of a series of equidistant peaks (q_n), the periodicity (d) of a lamellar phase was calculated using the equation $d=2n\pi/q_n$, n being the order of a diffraction peak attributed to the lamellar phase.

Statistical analysis

Statistical outcomes were determined using GraphPad Prism 5 (GraphpPad Software Inc, CA, USA). Two-way ANOVA tests were performed to analyze the FFA chain length distribution and paired student t-tests for mid-point transition temperature and LPP repeat distance.

Results

2nd and 3rd generation Ex-HSEs show a viable epidermis executing early and late epidermal differentiation programs

To determine the morphology and differentiation of the epidermis of the Ex-HSEs, the middle region, representing the main part of the outgrowths, was investigated. The original biopsies could always be passaged till the 2nd generation (age: 17-49 years). However, from 2 out of the 4 skin donors (age: 17 and 18 years), the 3rd generation Ex-HSE could be cultured.

The 2nd and 3rd generation Ex-HSEs display a fully stratified epidermis (figure 1). The expression of the early (keratin 10 (K10)), and late (filaggrin, loricrin and involucrin) differentiation markers was investigated to examine whether their expression changed during passaging. The outgrowths of the 2nd and 3rd generation showed the presence of K10, filaggrin and loricrin similar to the 1st generation and native human skin (figure 1, for explants see figure S3). Early and late differentiation programs were executed as demonstrated by the expression of K10 in all suprabasal epidermal layers and filaggrin and loricin in the stratum granulosum (SG). The expression of involucrin differed in the 2nd and 3rd generation outgrowths compared to the 1st generation. The 2nd generation outgrowth shows an intense involucrin staining in the SG, which extends weakly to the upper and lower stratum spinousum (SS) and 3rd generation outgrowths show evenly distributed involucrin expression over the entire epidermis. However, in the 1st generation outgrowth, involucrin expression is most pronounced in the SG and a weak staining is observed in the upper SS (figure 1).

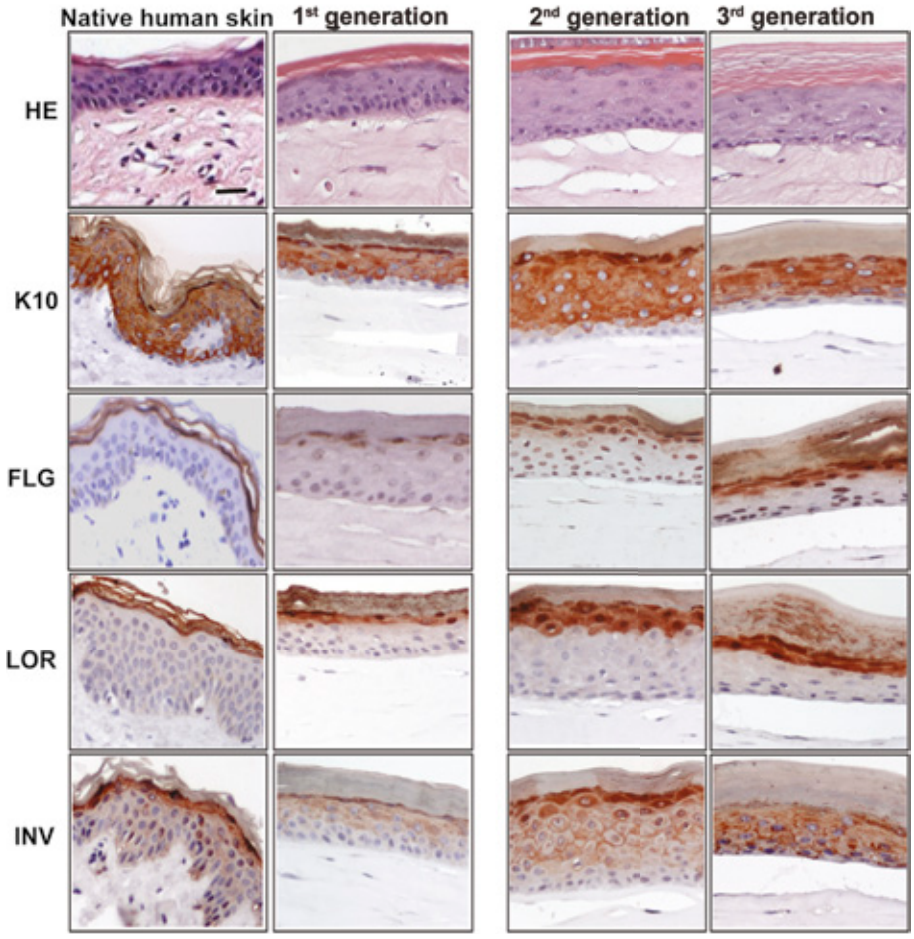

Figure 1: Cross sections of the outgrowth of 2nd and 3rd generation Ex-HSEs in comparison with the 1st generation Ex-HSEs and native human skin that are stained with haematoxylin/eosin (HE). Immunohistochemical staining of keratin 10 (K10), filaggrin (FLG), loricrin (LOR), involucrin (INV). 20x magnification, scale bar represents 30µm.

Orthorhombic lateral packing is gradually lost with increasing generations of Ex-HSEs

Our previous studies showed that the 1st generation Ex-HSEs do not fully maintain SC lipid properties as in native human skin (12). Therefore, we investigated whether passaging to the 2nd and 3rd generation results in SC lipid properties similar to the 1st generation. The lateral packing was examined in the Ex-HSEs by collecting FTIR spectra from 0°C-90°C, focusing on lipid chain CH_2 rocking vibrations. A hexagonal lipid organization is depicted by a single peak at 719 cm^{-1} and an orthorhombic lipid organization by two peaks at 719 cm^{-1} and 730 cm^{-1} in the FTIR spectrum.

At 0°C, 2nd generation explants show two contours at 719 cm^{-1} and 730 cm^{-1}. The 730 cm^{-1} peak disappears at 24.6±4.2°C. The lateral organization in the 3rd generation explants could not be detected due to a low IR signal. The 2nd and 3rd generation outgrowths only show a hexagonal packing (figure 2), as only the 719 cm^{-1} contour is present in the spectrum. When comparing the lateral packing in the 2nd generation explant with the 1st generation explant and native skin, the 1st generation explant and human skin also show two peaks with the 730 cm^{-1} peak more intense indicating a higher level of orthorhombic packing. The 730 cm^{-1} peak disappears at 47.3±3.1°C and 35.0±7.1°C for human skin and the 1st generation explant, respectively (data not shown for human skin). When focusing on the outgrowth, the FTIR spectrum of the 2nd generation outgrowth exhibits only one peak, reflecting only a hexagonal lateral packing, while the 1st generation outgrowth shows a small fraction of lipids in an orthorhombic packing which disappears at 30±8.5°C.

We also investigated the CH_2 symmetric stretching frequency to determine whether the conformational ordering of the lipid chains underwent changes during culture. In a crystalline organization, the chains are fully extended and the conformational order is high with CH_2 symmetric stretching frequencies below 2850 cm^{-1}. CH_2 symmetric stretching frequencies at 2852 cm^{-1} and higher indicate disordered chains, which is characteristic for a liquid phase. From the thermotropic response curves, the mid-point temperature at which the lipid domains change from a crystalline state to a liquid state was determined (for detailed explanation, see figure S4). This is referred to as "Mid-point transition temperature" (MTT). The MTT is significantly lower in the 2nd generation explants and outgrowths than in native human skin ($p<0.05$ and $p<0.01$ respectively, table S5). The CH_2 stretching frequency at skin temperature (32°C) was also higher in the 2nd generation outgrowths in comparison to native human skin (table S5, $p<0.05$). These results indicate an increased conformational disordering in the 2nd generation Ex-HSEs compared to native skin. However, the CH_2 stretching frequency at 32°C and MTT of the 2nd generation Ex-HSE was similar to the 1st generation. The MTT and CH_2 stretching frequency at skin temperature of the 3rd generation outgrowth was comparable to the 2nd generation outgrowth (table S5). However, this information could not be obtained for the 3rd generation explant due to low IR signal.

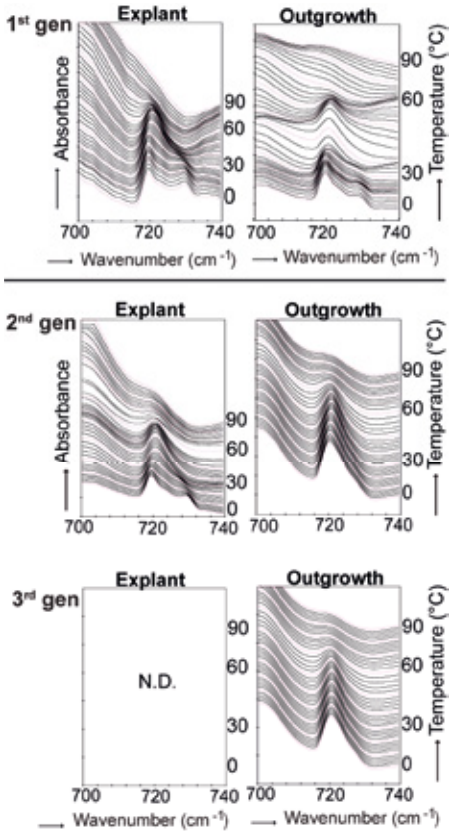

Figure 2: FTIR spectra showing the CH_2 rocking vibrations of 1st, 2nd and 3rd generation explants and outgrowths as a function of temperature (0°C-90°C). A hexagonal lipid organization is characterized by the presence of one peak at 719cm^{-1} at the CH_2 rocking band and an orthorhombic lipid packing by two peaks at 719cm^{-1} and 730cm^{-1}. Generation (gen), not determined (N.D.).

LPP is present in 2nd and 3rd generation Ex-HSEs

The lamellar lipid organization was examined in the explants and their corresponding outgrowths using SAXD. The diffraction profiles show three diffraction peaks denoted by 1, 2 and 3, indicating the 1st, 2nd and 3rd order diffraction peak of the LPP (figure S6). In addition, the diffraction profiles show the presence of crystalline CHOL domains similar to the phase separated CHOL in all Ex-HSEs and native human skin. No statistical significance in repeat distance of the LPP was observed between the 2nd and 3rd generation explants and outgrowths in comparison to the 1st generation (table S6).

2nd and 3rd generation Ex-HSEs contain the main SC lipid classes in native human skin

Since we observed changes in the lipid organization of the outgrowth, we examined the lipid composition because changes in the lipid composition are causative for changes in lipid organization. Firstly, we focused on the three main lipid classes, CERs, CHOL and FFAs (figure 3a). The main SC lipid classes were present

in the 2nd and 3rd generation outgrowths and no significant changes were observed in the band intensity of CERs and CHOL in the 2nd and 3rd generation compared to the 1st generation outgrowth and human skin. Compared to native skin, the intensity of the FFAs was reduced in the 2nd and 3rd generation outgrowths as was also observed in the 1st generation outgrowth (figure 3b, $p<0.05$). Secondly, the 2nd and 3rd generation show all CERs present in human SC as detected by HPTLC. The relative intensities of the ester linked ω-hydroxy (EO) CERs, CER EOS and CER EOP in the 2nd generation were similar to the 1st generation. However, CER EOS and CER EOP relative intensities in the 2nd generation were significantly higher than in native human skin (EOS: $p<0.01$ and EOP: $p<0.05$, figure 3c). No significant differences were observed in the relative intensity of the other CER subclasses when comparing the 2nd generation Ex-HSEs with the 1st generation and native human skin. Since CerS3 is involved in the synthesis of EO CERs (linking the sphingoid base to the ω-hydroxy fatty acid), its expression in the epidermis was analyzed by immunofluorescence. CerS3 is expressed weakly in supra-basal layers and intensely in the SG in native human skin (figure 3d). However, all Ex-HSE generations show an intense staining of CerS3 in all suprabasal layers.

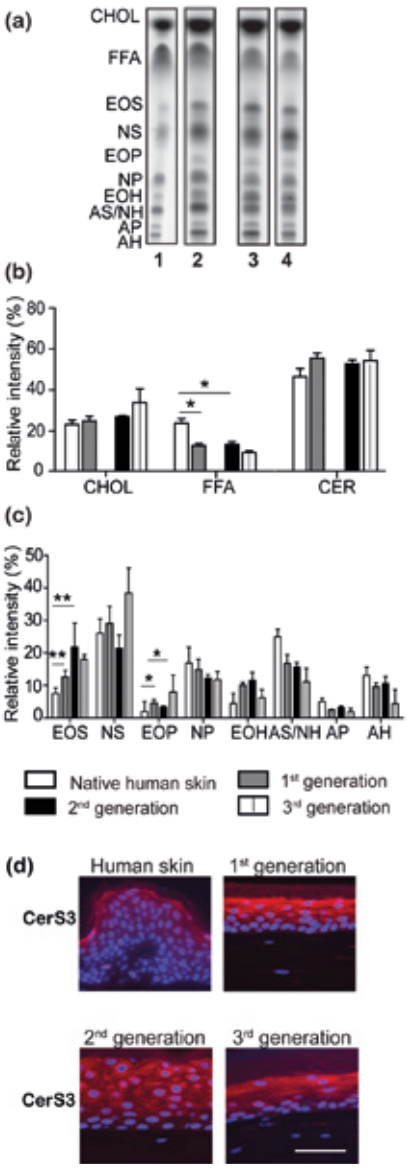

Figure 3: SC barrier lipids and ceramide synthase 3 (CerS3) expression in 1st, 2nd and 3rd generation outgrowths and native human skin. a) Lipid profiles from human skin and outgrowths of Ex-HSEs. Lane 1: Native human skin, Lane 2: 1st generation outgrowth, Lane 3: 2nd generation outgrowth, Lane 4: 3rd generation outgrowth. b) Relative intensity of the lipid bands of the main SC lipid classes. c) Relative distribution of the various CER subclasses d) CerS3 expression in Ex-HSEs and native human skin. 20x magnification, scale bar 50µm. Cholesterol (CHOL), free fatty acids (FFA), ceramides (CER). CERs are named according to the nomenclature by Motta et al., and Masukawa et al., (35, 36) (see table S4, paired student *t*-test, *p<0.05, **p<0.01). The data is presented as the mean ± standard deviation from four independent experiments.

2nd generation Ex-HSEs show a substantial level of unsaturated FFAs

HPTLC results revealed that the total FFA level was lower in the 2nd generation Ex-HSE compared to native human skin. To analyze the FFA composition in more detail, we examined the chain length distribution and saturation of the FFAs using LC-MS as this was not done in our previous study focusing on the 1st generation of Ex-HSE (12). The FFA chain lengths with C16-C18 were excluded from the analysis to avoid false positive results from sebaceous lipids and subcutaneous fat from native human skin.

Analysis of saturated FFAs (SFAs) and mono-unsaturated FFAs (MUFAs) showed that the 2nd generation contains relatively more MUFAs than SFA in contrast to native human skin (significance $p<0.05$, figure 4a, b) where the SFAs are always highly abundant compared to MUFAs. The abundance of MUFAs in the 2nd generation was not significantly different to that in the 1st generation.

The SFAs chain length in the 2nd generation outgrowths displays a normal distribution. The even chain length FFAs are more abundant than the odd chain lengths with FFA C24:0 and FFA C26:0 as the most predominant chain lengths. The relative level of long chain (C19:0-C22:0) SFAs was significantly higher in the 2nd generation than in native human skin (figure 4c; $p<0.05$). Furthermore, the consistent reduction in very long chain SFAs (C24:0-C28:0) in the 2nd generation was significant compared with native human skin (figure 4c; $p<0.01$). The chain length distribution of 2nd generation SFAs was similar to the 1st generation with the exception of ultra-long chain FFAs (≥C30:0). These were significantly reduced in the 2nd generation compared with the 1st generation (figure 4c).

The chain length distribution of MUFAs in the 2nd generation also shows that even chain lengths are more abundant than odd chain lengths with FFA C20:1 and FFA C24:1 as the most abundant. The relative level of MUFAs with chain lengths C19:1 till ≥C30:1 was significantly higher in the 2nd generation than in native human skin (figure 4d; $p<0.001$). No significant difference was observed in the MUFA chain length distribution between the 1st and 2nd generation.

The expression of stearoyl-CoA desaturase (SCD), a key enzyme in FFA unsaturation was analyzed. SCD is expressed in the stratum basale (SB) in native human skin. The 1st and 2nd generation outgrowths show SCD expression in the SB and SS while the 3rd generation expresses SCD in the entire viable epidermis (figure 4e).

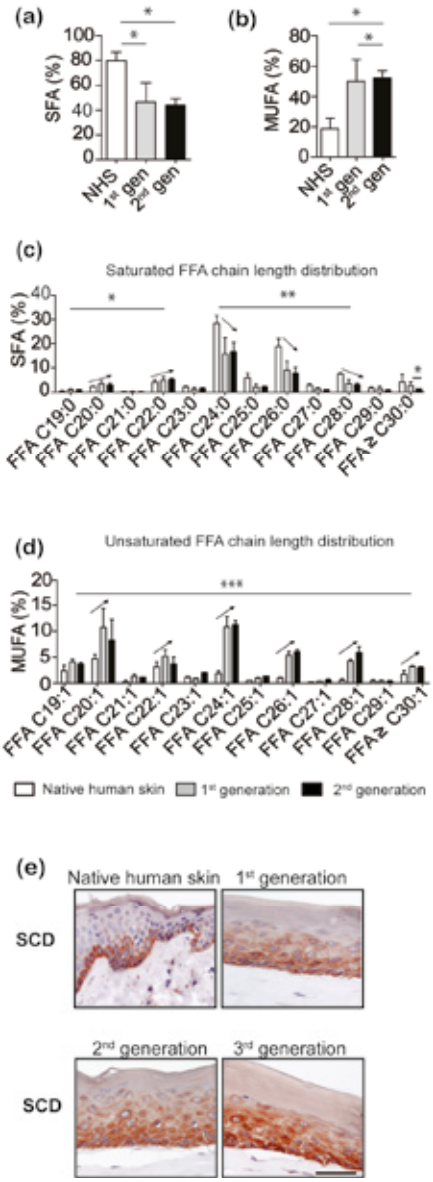

Figure 4: The relative level of a) saturated FFAs (SFAs) and b) mono-unsaturated FFAs (MUFAs) and the chain length distribution of c) SFAs and d) MUFAs in the native human skin, 1st generation outgrowths and 2nd generation outgrowths. e) expression of stearoyl-CoA desaturase (SCD) in Ex-HSEs and native human skin. In a and b the SFAs and MUFAs are displayed as a percentage of the total FFAs. c and d show the variations in the relative levels of the various SFAs chain lengths and MUFAs respectively in relation to the total FFA level (i.e. Total FFAs = SFAs+MUFAs = 100%). *p<0.05, **p<0.01, ***p<0.001. The data represented is shown as the mean ± standard deviation of four independent experiments. 20x magnification, scale bar represents 50µm. Native human skin (NHS), generation (gen).

Discussion

In this study, we investigated whether the tissue generated from the 1st generation Ex-HSEs can be further expanded by growing a 2nd generation and even a 3rd generation Ex-HSE. This method of generating epidermal tissue can be potentially useful for analysis that require larger amounts of skin. For example, in studies that involve skin diseases, the expansion of skin tissue eliminates the need to harvest several skin biopsies and provides a means to study the progression of skin diseases *in vitro* which cannot be performed *in vivo* e.g. investigating the invasive behavior of skin cancers.

The results show that it is possible to passage outgrowth from the 1st generation Ex-HSEs to establish 2nd and 3rd generations, which maintain morphology, differentiation process and lamellar lipid organization similar to the 1st generation. This shows that 40x (2nd generation, table S1) and 60x (3rd generation, table S1) expansion of 4mm biopsies can be achieved, which allows extensive characterization of the epidermal tissue and the SC barrier properties which cannot be performed with only a 4mm biopsy. However, only 50% of human skin biopsies could be used to establish the 3rd generation. This may be attributed to differences between donors influencing keratinocyte proliferation and differentiation, including age, genetic factors and lifestyle. Due to donor confidentiality, information regarding lifestyle and genetics could not be obtained. However, skin donors aged 17-18 years could be passaged to the 3rd generation and other skin donors ranging from 33-49 years could not. We also compared Ex-HSEs generated from younger skin donors (17-18 years) and an older skin donor (49 years old). In young donors, a similar proliferation index (PI) maintained from the 1st till the 3rd generation. In Ex-HSEs generated from the older skin donor (49 years), there is a 4x reduction in PI in the 2nd generation compared to the 1st generation Ex-HSEs (data not shown). This may contribute to the inability of this donor to be passaged towards the 3rd generation and is in line with previous studies in which age is associated with proliferation capacity and passaging of keratinocytes *in vitro* (21, 22). However, in order to fully explore these differences, the outgrowth of more old and young donors should be studied.

We observed that the expression of K10, filaggrin and loricrin were maintained in the 2nd and 3rd generation. However, involucrin expression gradually shifts to the SS and finally to the SB in the 3rd generation. This finding may result from changes in the STAT5a/PPAR-γ pathway as this pathway regulates involucrin expression in differentiating human keratinocytes (23). Suprabasal expression of involucrin in the epidermis has also been reported in other HSEs suggesting that culture conditions may influence the expression of involucrin *in vitro* (24, 25).

The studies presented here indicate that orthorhombic lipid organization is reduced when increasing the number of generations. Therefore the orthorhombic packing cannot be reproduced *in vitro* under conditions described in this study. Only a hexagonal lateral packing was observed in the 2nd and 3rd generation outgrowths, similar to other epidermal and full thickness HSEs (12, 25-27). The abundant formation of a hexagonal packing in culture may be explained by: a reduction in SC FFAs levels and in their chain lengths or by an increase in the relative levels of MUFAs (28).

The 2nd generation outgrowth showed a normal SFA chain length distribution although the relative level of SFAs was lower, and MUFAs higher than in native human skin. Furthermore the ultra-long chain SFAs (≥C30:0) were lower in the 2nd generation than the 1st generation outgrowths and human skin. This may contribute to the absence of the orthorhombic lateral packing in the 2nd generation outgrowths. The 3rd generation outgrowth was not analyzed by LC-MS due to its close similarity in lipid organization with the 2nd generation outgrowth. We expect similar lipid composition in both the 2nd and 3rd generation outgrowth since the lipid composition highly determines lipid composition. In contrast to the lateral packing, the LPP repeat distance can be maintained in all three Ex-HSE generations. Studies using model lipid systems also suggest that increased levels of MUFAs mainly affects the lateral packing while the lamellar phases are not changed (28). The increased MUFAs content in the 2nd generation Ex-HSEs and in other HSEs (29) in relation to native human skin might be related to the increased expression of SCD. In 2nd generation Ex-HSEs, the level of MUFAs is increased, especially the long chain MUFAs (C24:1-C28:1), whereas long chain SFAs levels (C24:0-C28:0) are decreased in comparison with native human skin. This suggests that FFA processing in the Ex-HSEs is skewed towards unsaturation probably due to increased SCD expression and/or activity (29). SCD-1 generates C16:1 and C18:1 from C16:0 and C18:0, respectively, after which most probably the unsaturated FFAs are elongated (30). We therefore hypothesize that in Ex-HSEs, most FFAs are first unsaturated and thereafter elongated. In the absence of measuring the abundance of C16:0 and 18:0 FFAs, the average chain length of the FFA was similar between the native human skin and the Ex-HSEs (data not shown), which suggests that the main difference in FFA profile is unsaturation.

The relative intensities of EO CERs in the HPTLC plates were increased in 1st until 3rd Ex-HSE generations and in other HSEs compared to native human skin (29). The formation of CERs in keratinocytes is partly dependent on ceramide synthases (CerS) which n-acylate FFAs to a sphingoid base. An increase in CerS activity or expression, especially CerS3 (which synthesizes very long chain CERs) may contribute to the increased EO CER levels (31). PPARß/δ and PPARγ may also play a role in the increased EO CERs in the outgrowths, because PPARß/δ and PPARγ activation stimulates CerS3 expression in human keratinocytes and increases EO CERs in the hairless mouse (32, 33). Furthermore, increased ω-acyl transferase (generates EO CERs from acid condensation of linoleic acid to ultra-long CERs) expression and the availability of very long chain FFAs could influence the levels of EO CERs in the outgrowths (34).

Investigation of the lipid properties with regards to age were also compared. Our data suggest that the average FFA chain length in 1st generation Ex-HSEs is not affected by age as no differences in average chain length were observed. However, the level of MUFAs relative to the total FFA is higher in 1st generation Ex-HSEs from the older skin donor (71%) compared to younger donors (40%). This is also reflected in the lipid organization of the 1st generation outgrowth. A higher fraction of lipids form an orthorhombic lateral packing in the 1st generation Ex-HSEs from the young donors than the lipids in the 1st generation Ex-HSE from the old donor (figure S7). Therefore, age might contribute to the lipid composition of Ex-HSEs. However, further studies are required to fully explore this.

In addition to the presented Ex-HSEs, we also examined outgrowth cultures derived from isolated human epidermal sheets. Before culturing, the epidermis of the native human skin was separated by dispase treatment and the epidermal sheet was placed onto the dermal equivalent. 2nd and 3rd generation HSEs were also generated and with similar epidermal differentiation as in Ex-HSEs (figure S5) as well as the lipid properties (data not shown).

We conclude from this study that expansion of 4mm skin biopsies on a dermal equivalent to the 2nd or 3rd generation, depending on the skin donor, can serve as a method to expand valuable skin material in order to analyze morphological and differentiation parameters as in the native epidermis. Some aspects of the lipid organization and composition of native human skin is not reproduced in 2nd and 3rd generation Ex-HSEs, which should be considered when performing barrier function studies.

Acknowledgements

The authors thank the personnel at the DUBBLE beam line (BM26), ESRF for their support with the x-ray measurements. This research was financially supported by Dutch Technology Foundation STW (grant no. 10703).

References

1. Semlin L, Schäfer-Korting M, Borelli C, Korting HC: *in vitro* models for human skin disease. Drug Discov Today 16: 132-139, 2011.
2. Engelhart K, El Hindi T, Biesalski H-K, Pfitzner I: *in vitro* reproduction of clinical hallmarks of eczematous dermatitis in organotypic skin models. Arch Dermatol Res 297: 1-9, 2005.
3. Commandeur S, De Gruijl FR, Willemze R, Tensen CP, El Ghalbzouri A: An *in vitro* three-dimensional model of primary human cutaneous squamous cell carcinoma. Exp Dermatol 18: 849-856, 2009.
4. Shakespeare PG: The role of skin substitutes in the treatment of burn injuries. Clin Dermatol 23: 413-418, 2005.
5. Supp DM, Boyce ST: Engineered skin substitutes: practices and potentials. Clin Dermatol 23: 403-412, 2005.
6. Garlick JA: Engineering Skin to Study Human Disease - Tissue Models for Cancer Biology and Wound Repair. In Tissue Engineering II. Edited by Lee K, Kaplan D. Springer Berlin Heidelberg, 2007. pp. 207-239.
7. Netzlaff F, Lehr CM, Wertz PW, Schaefer UF: The human epidermis models EpiSkin®, SkinEthic® and EpiDerm®: An evaluation of morphology and their suitability for testing phototoxicity, irritancy, corrosivity, and substance transport. Eur J Pharm Biopharm 60: 167-178, 2005.
8. El Ghalbzouri A, Siamari R, Willemze R, Ponec M: Leiden reconstructed human epidermal model as a tool for the evaluation of the skin corrosion and irritation potential according to the ECVAM guidelines. Toxicol *in vitro* 22: 1311-1320, 2008.
9. Gibbs S: *in vitro* Irritation Models and Immune Reactions. Skin Pharmacol Physiol 22: 103-113, 2009.
10. El Ghalbzouri A, Jonkman M, Kempenaar J, Ponec M: Recessive Epidermolysis Bullosa Simplex Phenotype Reproduced *in Vitro*: Ablation of Keratin 14 Is Partially Compensated by Keratin 17. Am J Pathol 163: 1771-1779, 2003.
11. Coulomb B, Saiag P, Bell E, Breitburd F, Lebreton C, Heslan M, et al.: A new method for studying epidermalization *in vitro*. Br J Dermatol 114: 91-101, 1986.
12. Thakoersing VS, Danso MO, Mulder A, Gooris G, El Ghalbzouri A, Bouwstra JA: Nature versus nurture: does human skin maintain its stratum corneum lipid properties *in vitro*? Exp Dermatol 21: 865-870, 2012.
13. Bouwstra J, Gooris GS, van der Spek J, Bras W: Structural investigations of human stratum corneum by small-angle X-ray scattering. J Invest Dermatol 97: 1005-1012, 1991.
14. Bouwstra J, Pilgram G, Gooris G, Koerten H, Ponec M: New Aspects of the Skin Barrier Organization. Skin Pharmacol Physiol 14(suppl 1): 52-62, 2001.
15. Damien F, Boncheva M: The Extent of Orthorhombic Lipid Phases in the Stratum Corneum Determines the Barrier Efficiency of Human Skin *In Vivo*. J Invest Dermatol 130: 611-614, 2009.
16. Bouwstra JA, Groenink HWW, Kempenaar JA, Romeijn SG, Ponec M: Water Distribution and Natural Moisturizer Factor Content in Human Skin Equivalents Are Regulated by Environmental Relative Humidity. J Invest Dermatol 128: 378-388, 2008.

17. Ponec M, Weerheim A, Kempenaar J, Mulder A, Gooris GS, Bouwstra J, et al.: The Formation of Competent Barrier Lipids in Reconstructed Human Epidermis Requires the Presence of Vitamin C. J Invest Dermatol 109: 348-355, 1997.
18. Smola H, Thiekötter G, Fusenig N: Mutual induction of growth factor gene expression by epidermal-dermal cell interaction. J Cell Biol 122: 417-429, 1993.
19. de Jager M, Groenink W, Bielsa i Guivernau R, Andersson E, Angelova N, Ponec M, et al.: A Novel *in vitro* Percutaneous Penetration Model: Evaluation of Barrier Properties with & P-Aminobenzoic Acid and Two of Its Derivatives. Pharm Res 23: 951-960, 2006.
20. Bligh EG, Dyer WJ: A rapid method of total lipid extraction and purification. Can J Biochem Physiol 37: 911-917, 1959.
21. Gilchrest BA: *in vitro* Assessment of Keratinocyte Aging. J Investig Dermatol 81: 184s-189s, 1983.
22. Rheinwald JG GH: Serial cultivation of strains of human epidermal keratinocytes: the formation of keratinizing colonies from single cells. Cell 6: 331-343, 1975.
23. Dai X, Sayama K, Shirakata Y, Hanakawa Y, Yamasaki K, Tokumaru S, et al.: STAT5a/PPARgamma. Pathway Regulates Involucrin Expression in Keratinocyte Differentiation. J Invest Dermatol 127: 1728-1735, 2007.
24. Boelsma E GS, Faller C, Ponec M: Characterization and comparison of reconstructed skin models: morphological and immunohistochemical evaluation. Acta Derm Venereol 80: 82-88, 2000.
25. Thakoersing V, Gooris G, Mulder A, Rietveld M, El Ghalbzouri A, Bouwstra J: Unraveling barrier properties of three different in-house human skin equivalents. Tissue Eng Part C: Methods 18: 1-11, 2012
26. Bouwstra JA, Gooris GS, Weerheim A, Kempenaar J, Ponec M: Characterization of stratum corneum structure in reconstructed epidermis by X-ray diffraction. J Lipid Res 36: 496-504, 1995.
27. Tfayli A, Bonnier F, Farhane Z, Libong D, Byrne HJ, Baillet-Guffroy A: Comparison of Structure and organization of cutaneous lipids in a reconstructed skin model and human skin: spectroscopic imaging and chromatographic profiling. Exp Dermatol 23: 441-443, 2014.
28. Mojumdar EH, Helder RWJ, Gooris G, Bouwstra JA: Monounsaturated fatty acids reduce the barrier of stratum corneum lipid membranes by enhancing the formation of a hexagonal lateral packing. Langmuir 30: 6534-6543, 2014.
29. Thakoersing V, van Smeden J, Mulder A, Vreeken R, El Ghalbzouri A, Bouwstra J: Increased Presence of Monounsaturated Fatty Acids in the Stratum Corneum of Human Skin Equivalents. J Invest Dermatol 133: 59-67, 2013.
30. Ohno Y, Suto S, Yamanaka M, Mizutani Y, Mitsutake S, Igarashi Y, et al.: ELOVL1 production of C24 acyl-CoAs is linked to C24 sphingolipid synthesis. Proc Natl Acad Sci USA 107: 18439-18444, 2010.
31. Jennemann R, Rabionet M, Gorgas K, Epstein S, Dalpke A, Rothermel U, et al.: Loss of ceramide synthase 3 causes lethal skin barrier disruption. Hum Mol Genet 21: 586-608, 2012.
32. Mizutani Y, Sun H, Ohno Y, Sassa T, Wakashima T, Obara M, et al.: Cooperative Synthesis of Ultra Long-Chain Fatty Acid and Ceramide during Keratinocyte Differentiation. PLoS ONE 8: e67317, 2013.
33. Man M-Q, Choi E-H, Schmuth M, Crumrine D, Uchida Y, Elias PM, et al.: Basis for Improved

Permeability Barrier Homeostasis Induced by PPAR and LXR Activators: Liposensors Stimulate Lipid Synthesis, Lamellar Body Secretion, and Post-Secretory Lipid Processing. J Invest Dermatol 126: 386-392, 2006.

34. Rabionet M, Gorgas K, Sandhoff R: Ceramide synthesis in the epidermis. Biochim Biophys Acta-Molecular and Cell Biology of Lipids 1841: 422-434, 2014.
35. Motta S, Monti M, Sesana S, Caputo R, Carelli S, Ghidoni R: Ceramide composition of the psoriatic scale. Biochim Biophys Acta-Molecular basis of disease 1182: 147-151, 1993.
36. Masukawa Y, Narita H, Shimizu E, Kondo N, Sugai Y, Oba T, et al.: Characterization of overall ceramide species in human stratum corneum. J Lipid Res 49: 1466-1476, 2008.

Supplementary figures

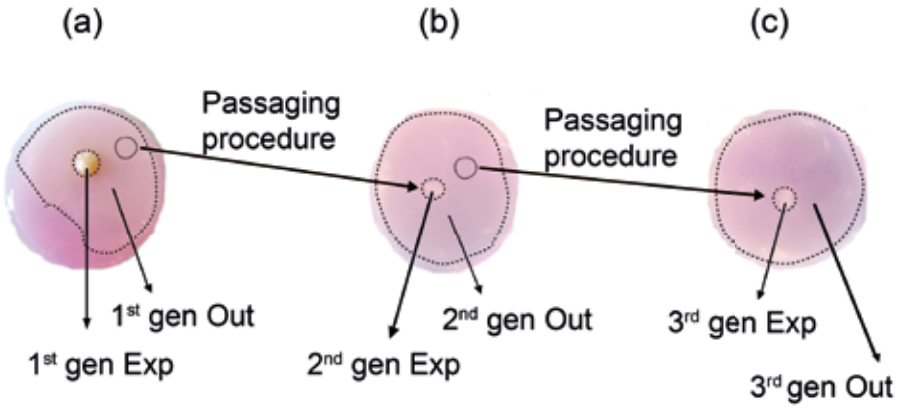

Figure S1: Generation of Ex-HSEs. A 4mm full thickness biopsy from native human skin is placed onto a fibroblast populated collagen matrix. This allows the epidermal cells to migrate and cover the surface of the collagen matrix and establish the 1st generation Ex-HSE (a). A small fragment of the 1st generation Ex-HSE is placed onto a new fibroblast populated collagen matrix to generate the 2nd generation Ex-HSE (b). A similar procedure is repeated with the 2nd generation Ex-HSE to generate the 3rd generation Ex-HSE (c). Generation (gen), explant (exp), outgrowth (out).

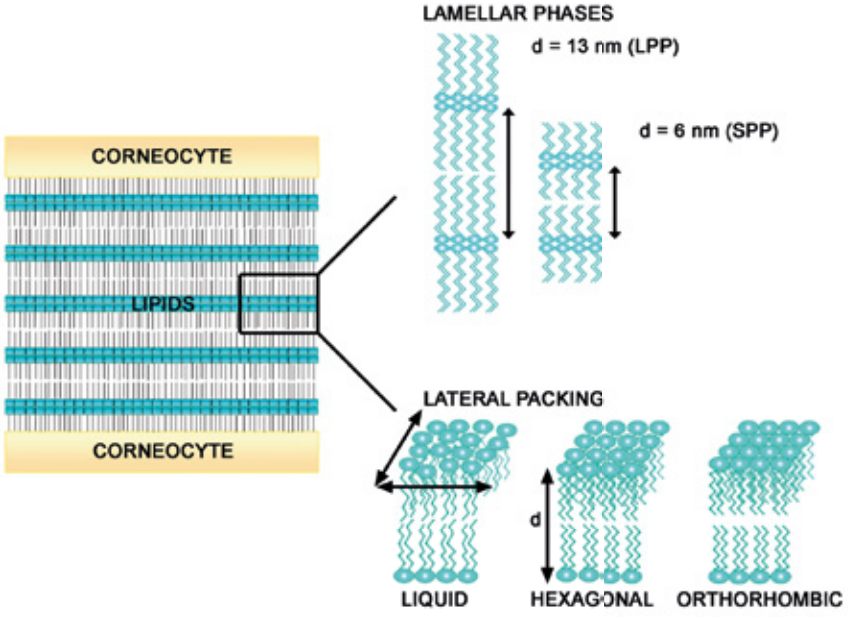

Figure S2: Lipid organization in human stratum corneum

The stratum corneum (SC), the outermost part of the epidermis consists of corneocytes which are surrounded by an organized intercellular lipid matrix. The lipids are organized in two lamellar phases: the long periodicity phase (LPP) and the short periodicity (SPP) phase with a repeat distance of 12nm and 6nm respectively. The lipids are also organized in the plane perpendicular to the lamellar organization which is referred to as lateral lipid organization. The lipids can be arranged in a liquid (disordered), hexagonal (less dense and ordered) and an orthorhombic (very dense and ordered) organization. This figure is adapted from Thakoersing et al., (1)

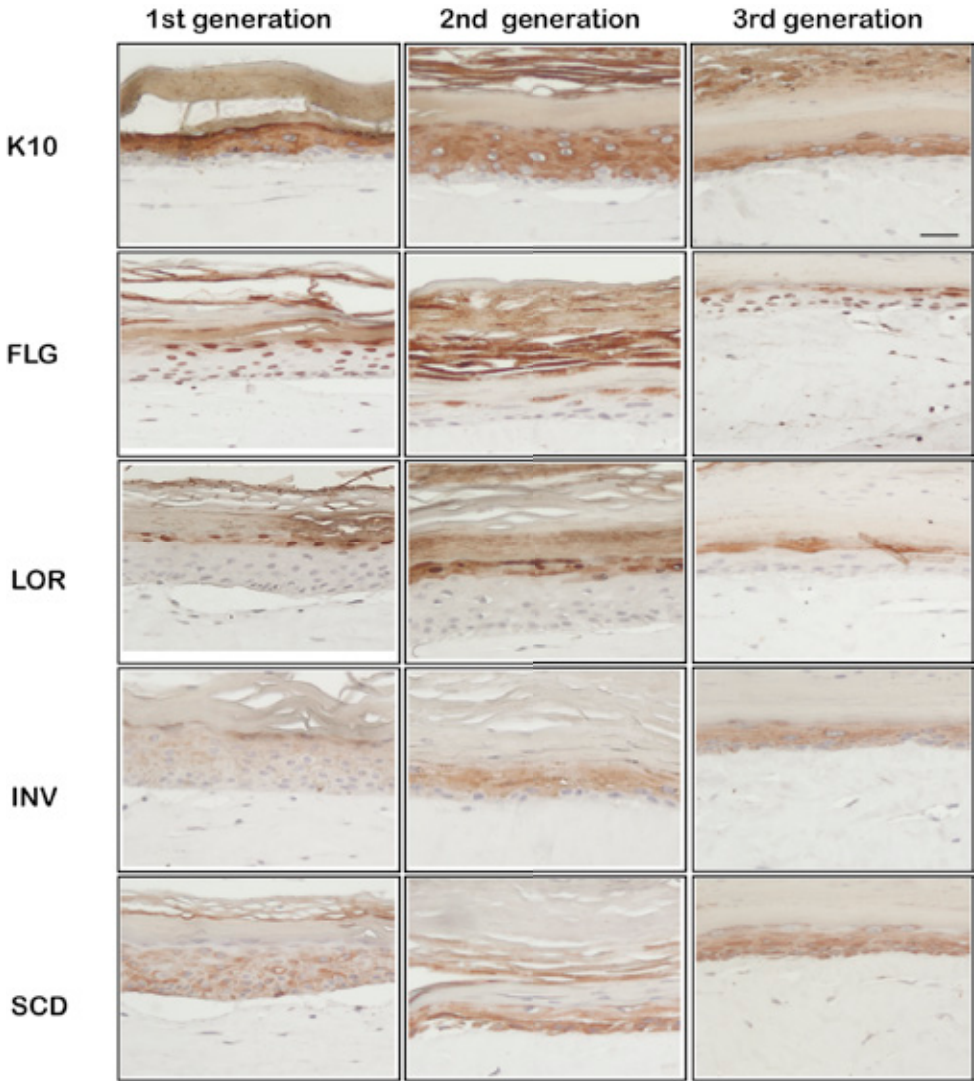

Figure S3: Immunohistochemical staining of the explants from 1st, 2nd and 3rd generation Ex-HSEs that are stained for keratin 10 (K10), filaggrin (FLG), loricrin (LOR), involucrin (INV) and stearoyl-CoA desaturase (SCD). Scale bar represents 30µm, 20x magnification.

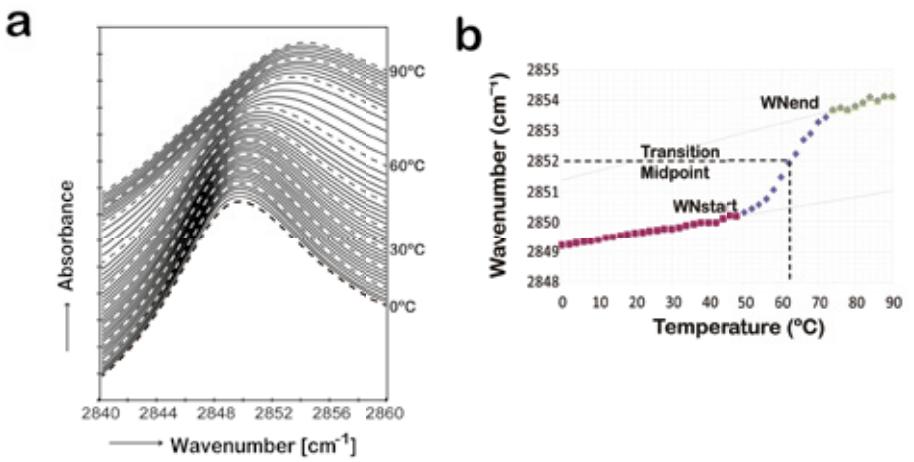

Figure S4: a) The stretching vibrations of the FTIR spectra from a representative Ex-HSE explant is shown as a function of temperature. In a crystalline packing, the chains are fully extended, the conformational order of the chains are high and this reflected by low CH_2 stretching frequencies less than 2850cm^{-1} (peak centre). Disordered chains, which is characteristic for a liquid phase have CH_2 symmetric stretching frequencies of 2852cm^{-1} and higher. b) Illustrates the procedure used to calculate the midpoint of the crystalline to liquid transition using the CH_2 stretching vibrations of the lipids. The midpoint transition temperature (MTT) is calculated as the mean of the last wavenumber at the beginning (WN_{start}) of the transition and the first wave number at the end of the transition (WN_{end}). The wavenumbers at the beginning and the end of the transition are determined by linear regression. The temperature at this calculated wavenumber is referred to as the MTT.

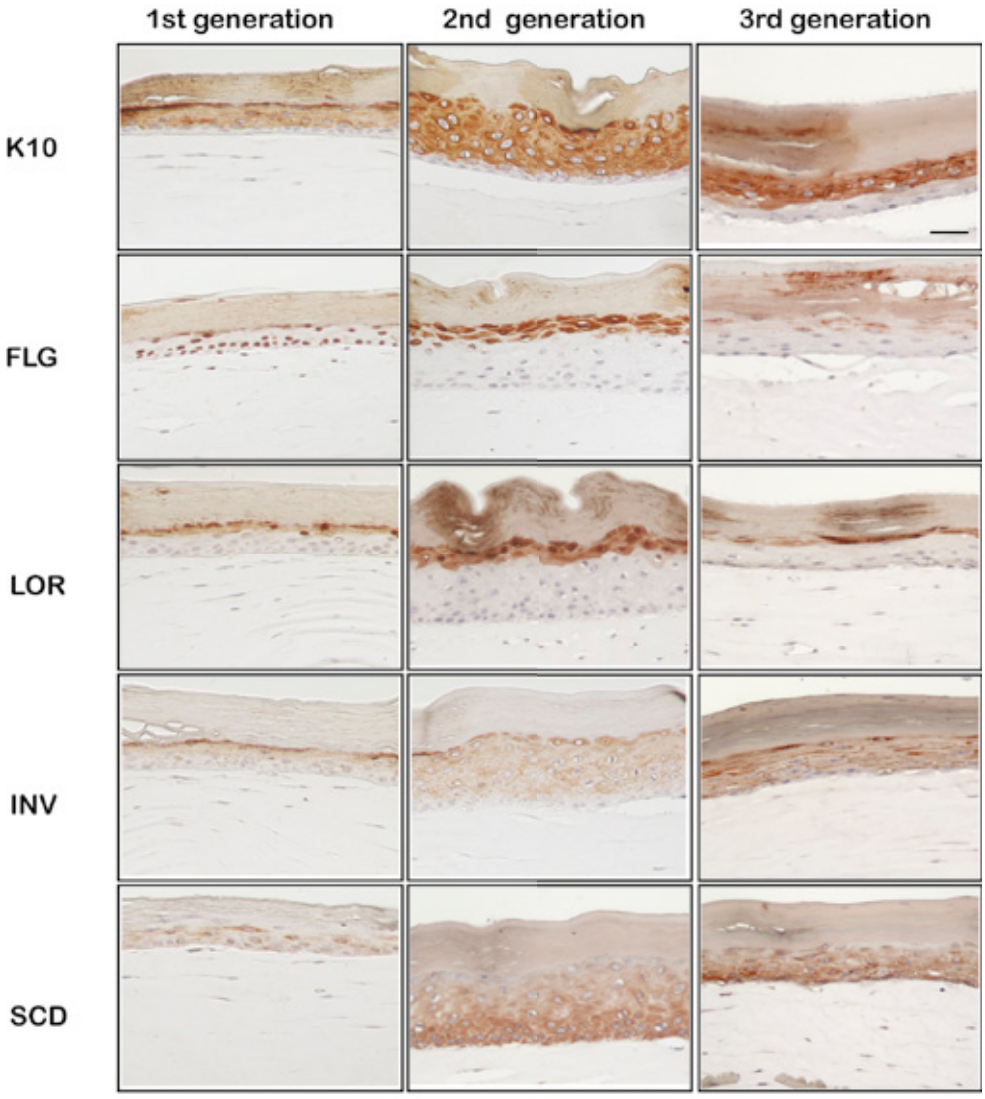

Figure S5: Immunohistochemical staining of the outgrowth of 1st, 2nd and 3rd generation epidermal sheet outgrowth HSEs for keratin 10 (K10), filaggrin (FLG), loricrin (LOR), involucrin (INV) and stearoyl-CoA desaturase (SCD). Scale bar represents 30µm, 20x magnification.

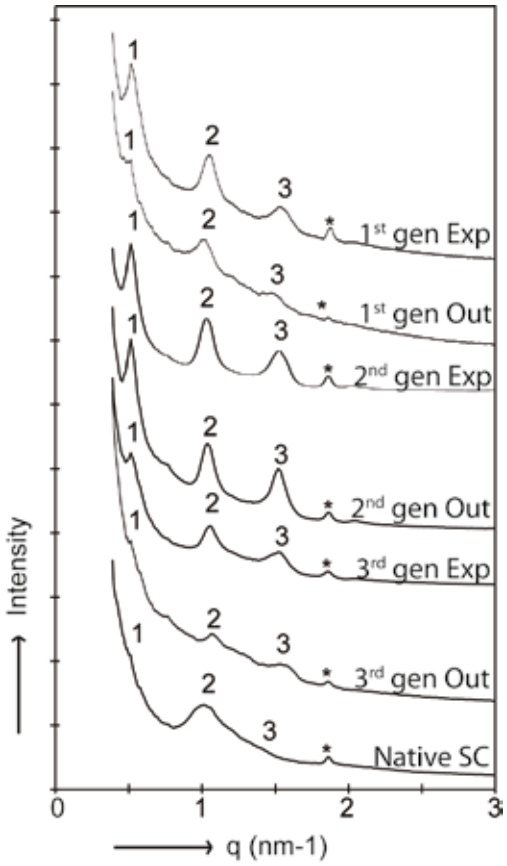

Figure S6: Representative diffraction pattern of SC from 1st , 2nd and 3rd generation explants and outgrowth. The 1st, 2nd and 3rd order of the LPP are indicated as 1, 2 and 3 respectively. The peak denoted by 2 in the diffraction pattern of native human SC is not only based on the 2nd order of the LPP, but also the 1st order SPP demonstrated by the increased width of this peak (2). Consequently, the repeat distance of the LPP and SPP in native human SC cannot be calculated directly from this diffraction profile. Crystalline cholesterol is indicated by (*). Generation (gen), explant (exp), outgrowth (out).

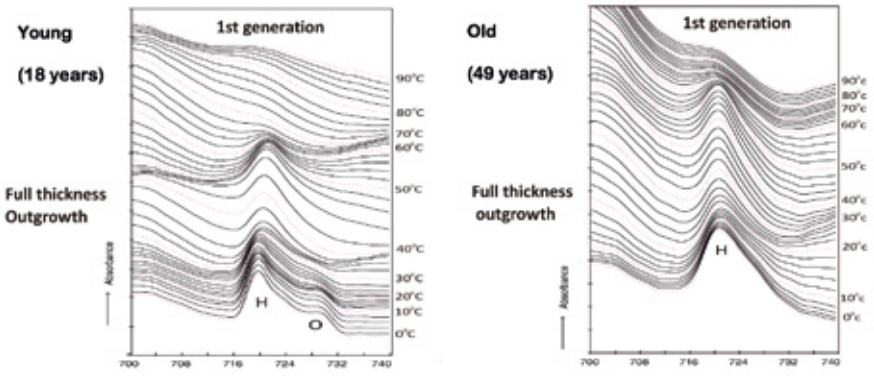

Figure S7: FTIR spectra showing the CH_2 rocking vibrations of 1st generation outgrowths as a function of temperature (0°C-90°C) from young and old skin donors. A hexagonal lipid organization is characterized by the presence of one peak at 719cm^{-1} at the CH_2 rocking band and an orthorhombic lipid packing by two peaks at 719cm^{-1} and 730cm^{-1}.

Supplementary tables

Table S1: Epidermal outgrowth in Ex-HSEs

Ex-HSE	**Average outgrowth area** (cm^2)	**Increase in epidermal material** (compared to 4mm biopsy)
Original biopsy	0.127	0
1st generation	2.543	20x
2nd generation	2.543	40x
3rd generation	2.543	60x

Table S2: Primary and secondary antibodies for immunohistochemical staining

Antibodies	Clone	Dilution	Company
Primary antibodies			
Mouse cytokeratin 10 Ab-2	DE-K10	1:800	Neomarkers, USA
Mouse filaggrin Ab-1	FLG01	1:800	Neomarkers, USA
Rabbit Loricrin	AF62	1:1200	Covance, USA
Mouse involucrin	SY5	1:1200	Sanbio, The Netherlands
Rabbit SCD	Polyclonal	1:100	Sigma-Aldrich
Rabbit ceramide synthase 3 (IF)	Polyclonal	1:75	Sigma Aldrich
Rabbit Ki67	SP6	1:800	Neomarkers, USA
Secondary antibody			
Biotinylated universal antibody, anti-rabbit/mouse IgG			Vector laboratories Burlingame, CA, USA
Rhodamine Red-X (Goat anti-rabbit) (IF)		1:300	Jackson immunoresearch Laboratory, USA

Table S4: Ceramide nomenclature

Eluent	Composition (v/v)	Distance (mm)
1	Dichloromethane/Ethylacetate/Acetone/Methanol (88:8:4:1)	40
2	Chloroform/Acetone/Methanol (76:8:16)	10
3	Hexane/Chloroform/Acetone/Methanol (6:80:12:2)	70
4	Hexane/Chloroform/Hexyl acetate/Acetone/Methanol (6:80:0.1:10:4)	95

The ceramides in human stratum cornuem contain one of these 4 sphingoid bases (dihydrosphingosine (dS), Sphingosine (S), phytosphingosine (P) and 6-hydroxy sphingosine (H)) and one of three acyl chains (non-hydroxy fatty acid (N), α-hydroxy fatty acid (A) and esterified ω-hydroxy fatty acid (EO)). These result in the 12 ceramide subclasses known to be present in human stratum corneum.

Table S5: Midpoint transition temperature and CH_2 symmetric stretching at 32°C in Ex-HSEs

Midpoint transition temperature (°C)			CH_2 symmetric stretching (cm^{-1}) at 32°C	
Ex-HSE	Explants	Outgrowth	Explants	Outgrowth
1st generation	60.7 ± 6.4	58.5 ± 7.6 *	2849.8 ± 0.4	2849.8 ± 0.2
2nd generation	58.5 ± 0.7 *	55.4 ± 7.3 **	2849.9 ± 0.7	2850.0 ± 0.2 *
3rd generation	N.D.	56.0 ± 2.8	N.D.	2850.1 ± 0.0
Native human SC	73.5 ± 1.8		2849.5 ± 0.1	

Paired student *t*-test was performed to determine significance between the native human SC and the Ex-HSEs (**p<0.01, *p<0.05), not determined (N.D.).

Table S6: Repeat distance of the LPP in the 1st - 3rd generation explants and outgrowths.

	Explants	Outgrowth
Ex-HSE	**LPP repeat distance (d)**	**LPP repeat distance (d)**
1st generation	12.1 ± 0.3nm	12.1 ± 0.4nm
2nd generation	11.9 ± 0.5nm	11.8 ± 0.4nm
3rd generation	11.6 ± 0.6nm	11.4 ± 0.4nm

Note: LPP in native human skin is ~13nm (2)

Supplementary materials and methods

Morphology and Immunohistochemistry

The primary and secondary antibodies are listed in table A2. The sections were incubated in sodium citrate buffer (pH 6) at 95°C for antigen retrieval. After cooling, the sections were blocked with normal horse serum (Vector laboratories Burlingame, CA) and incubated with the primary antibody diluted in 1% PBS/bovine serum albumin (BSA) overnight at 4°C.

Staining procedure with amino-ethylcarbazole: Sections were incubated with the secondary antibody (Vector laboratories Burlingame, CA) for 30 minutes and thereafter with the ABC reagent (Vector laboratories Burlingame, CA) for 30 minutes. The sections were washed with 0.1M sodium acetate buffer and subsequently in amino-ethylcarbazole (Sigma) dissolved in N,N-dimethylformamide (1g/250mL) (Sigma) with 0.1% hydrogen peroxide. All sections were counterstained with haematoxylin.

Immunofluorescence analyses: Sections were incubated with the secondary antibody for 1 hour and mounted using DAPI Vectashield (Vector laboratories Burlingame, CA).

Lipid analysis

High performance thin layer chromatography (HPTLC): Extracted lipids were analyzed by HPTLC as described previously (3). The solvents and running distances are provided in table A3. Co-chromatography of a standard lipid mixture was performed to identify the different lipid classes. The standard mixture contained free fatty acids (cerotic acid, tricosanoic acid, behenic acid, arachidonic acid, stearic acid, lignoceric acid, palmitic acid), cholesterol (Sigma) and ceramides (EOS, EOP, NS, NP, AS and AP, Cosmoferm, The Netherlands). The ceramide nomenclature is according to the terminology of Motta et al.,(4) and Masukawa et al.,(5) (table A4).

Reverse-phase liquid chromatography mass spectrometry (LC-MS): LC-MS analysis of FFA species was performed according to van Smeden et al., (6). An Alliance 2695 HPLC (Waters Corp. Milford, MA) was attached to a TSQ Quantum mass spectrometer (Thermo Finnigan, San Jose, CA, USA) which measured in atmospheric-pressure chemical ionization (APCI) mode. The analysis was performed in negative ionization mode with a scan range of 200-600 amu. The source heater temperature was set at 450°C, and heated capillary at 250°C and the discharge current at 5 μA. The total sample lipid concentration was 1mg/mL with an injection volume of 10 μL. FFA separation was achieved using a LiChroCART Purospher STAR analytical column (55 x 2 mm i.d. Merck, Darmstadt, Germany) under a flow rate of 0.6 mL/min using a binary gradient solvent system of acetonitrile/H_2O (90:10) to methanol/heptane (90:10). The analysis was performed using Xcalibur software version 2.0. The FFA chain lengths with C16-C18 were excluded from the analysis to avoid false positive results from sebaceous lipids and subcutaneous fat from native human skin.

References

1. Thakoersing V S, Danso M O, Mulder A, Gooris G, El Ghalbzouri A, Bouwstra J A. Nature versus nurture: does human skin maintain its stratum corneum lipid properties *in vitro*? Exp Dermatol 2012: 21: 865-870.
2. Bouwstra J, Gooris G S, Spek v d, Bras W. Structural investigations of human stratum corneum by small-angle X-ray scattering. J Invest Dermatol 1991: 97: 1005-1012.
3. Ponec M, Weerheim A, Lankhorst P, Wertz P. New acylceramide in native and reconstructed epidermis. J Invest dermatol 2003: 120: 581-588.
4. Motta S, Monti M, Sesana S, Caputo R, Carelli S, Ghidoni R. Ceramide composition of the psoriatic scale. Biochim Biophys Acta-Molecular basis of disease 1993: 1182: 147-151.
5. Masukawa Y, Narita H, Shimizu E, et al. Characterization of overall ceramide species in human stratum corneum. J Lipid Res 2008: 49: 1466-1476.
6. van Smeden J, Janssens M, Gooris G S, Bouwstra J A. The important role of stratum corneum lipids for the cutaneous barrier function. Biochimica et Biophysica Acta (BBA) - Molecular and Cell Biology of Lipids 2014: 1841: 295-313.